Nucleic Acids Research, 1994, Vol. 22, No. 23 5031–5037

Histidylation by yeast HisRS of tRNA or tRNA-like structure relies on residues −1 and 73 but is dependent on the RNA context

Joëlle Rudinger, Catherine Florentz and Richard Giegé*
Unité Propre de Recherche 9002 'Structure des Macromolécules Biologiques et Mécanismes de Reconnaissance', Institut de Biologie Moléculaire et Cellulaire du Centre National de la Recherche Scientifique, 15 rue René Descartes, F-67084 Strasbourg Cedex, France

Received August 5, 1994; Revised and Accepted October 26, 1994

ABSTRACT

Residue G_{-1} and discriminator base C_{73} are the major histidine identity elements in prokaryotes. Here we evaluate the importance of these two nucleotides in yeast histidine aminoacylation identity. Deletion of G_{-1} in yeast $tRNA^{His}$ transcript leads to a drastic loss of histidylation specificity (about 500-fold). Mutation of discriminator base A_{73}, common to all yeast $tRNA^{His}$ species, into G_{73} has a more moderate but still significant effect with a 22-fold decrease in histidylation specificity. Changes at position 36 in the anticodon loop has negligible effect on histidylation. The role of residues −1 and 73 for specific aminoacylation by yeast HisRS was further investigated by studying the histidylation capacities of seven minihelices derived from the Turnip Yellow Mosaic Virus tRNA-like structure. Changes in the nature of nucleotides −1 and 73 modulate this activity but do not suppress it. The optimal mini-substrate for HisRS presents a G·A mismatch at the position equivalent to residues G_{-1}·A_{73} in yeast $tRNA^{His}$, confirms the importance of this structural feature in yeast histidine identity. The fact that the minisubstrates contain a pseudoknot in which position −1 is mimicked by an internal nucleotide from the pseudoknot highlights further the necessity of a stacking interaction of this position over the amino acid accepting branch of the tRNA during the aminoacylation process. Individual transplantation of G_{-1} or A_{73} into yeast $tRNA^{Asp}$ transcript improves the histidylation efficiency of the engineered $tRNA^{Asp}$. However, a $tRNA^{Asp}$ transcript presenting simultaneously both residues G_{-1} and A_{73} becomes a less good substrate for HisRS, suggesting the importance of the structural context and/or the presence of anti-determinants for an optimal expression of these two identity elements.

INTRODUCTION

It is at present a well accepted view that specific aminoacylation of transfer ribonucleic acids (tRNAs) is mediated by a small set of identity nucleotides that most often interact with the cognate aminoacyl-tRNA synthetase (aaRS) and, by negative signals that prevent the tRNAs to be aminoacylated by non-cognate synthetases. Major identity nucleotides are known for all *Escherichia coli* tRNAs and several tRNAs in the eukaryotic kingdom [reviewed in e.g. (1–3)]. Much less is known about negative signals that have only been described explicitly in a few systems. In some cases, they have been correlated with the presence of modified nucleotides (4, 5). Expression of these identity elements are often modulated by structural elements present within the tRNA architecture (6–10). Identity nucleotides are searched *in vitro* by comparison of the aminoacylation capacities of wild-type and mutated tRNAs. Explicit proof of the contribution of nucleotides to identity comes from transplantation experiments in which the putative elements are inserted in a new tRNA framework with the expectation that the chimeric molecule acquires the new specificity. Optimal catalytic efficiency is obtained if no conformational or sequence context effects interfere with the expression of the specificity in the transplanted molecule.

Residues required for specifying histidylation in tRNAs have already been investigated in *E.coli* by both *in vitro* and *in vivo* approaches. Residue G_{-1}, only present in $tRNA^{His}$ species, and the discriminator base C_{73} specific for prokaryotic histidine tRNAs, have been found crucial for this identity (11, 12). The importance of these two residues, which likely are paired, was confirmed by the capacity of a microhelix derived from the amino acid acceptor arm of *E.coli* $tRNA^{His}$ containing base-pair G_{-1}·C_{73} to be histidylated, indicating also that the anticodon branch is not essential for *E.coli* histidyl-tRNA synthetase (HisRS) (13). Introduction of G_{-1} and C_{73} into a microhelix derived from $tRNA^{Ala}$ allowed its efficient histidylation, confirming the importance of this unique base-pair in histidylation identity. However, further transplantations of this element into

*To whom correspondence should be addressed

other microhelices showed that its expression is modulated by the sequence context of the microhelix, and particularly by the 2·71 and 3·70 base-pairs which are minor histidine determinants (14).

Although all $tRNA^{His}$ molecules sequenced to date present a residue G_{-1} (with one exception) (15), the explicit involvement of this residue in histidine identity has not been proven in organisms other than *E.coli*. Moreover, the nature of the discriminator base in $tRNA^{His}$ is different in prokaryotes and eukaryotes, so that it can be questioned about the uniqueness of histidine identity rules in living kingdoms. In this paper, we consider the case of yeast HisRS. Besides its cognate tRNA, this enzyme charges also viral tRNA-like structures (16–20) as well as a pseudoknot-containing minihelix recapitulating the amino acid acceptor branch of the Turnip Yellow Mosaic Virus (TYMV) tRNA-like structure (18).

Here we describe the histidylation capacities of a series of RNA transcripts derived from yeast $tRNA^{His}$, yeast $tRNA^{Asp}$ and TYMV RNA. Our data indicate that in both tRNA and tRNA-like structural frameworks, the coupling between discriminator nucleotide N_{73} and residue G_{-1}, or its mimick, governs histidine identity toward the yeast enzyme.

MATERIALS AND METHODS

Materials

Yeast HisRS was an enzyme preparation enriched by chromatographies on DEAE-cellulose, hydroxyapatite and phosphocellulose (21). T7 RNA polymerase was prepared from an overproducing strain harbouring plasmid pBl21 according to (22). L-[^{14}C] histidine (300 mCi/mmol) was from Amersham France (Les Ulis) and ajusted to a specific activity of 400 cpm/pmol with unlabelled aminoacid. Restriction enzymes *Bst*N1 and *Eco*T22I were purchased from New England Biolabs (Beverly, MA, USA) and United States Biochemical Corporation (Cleveland, OH, USA) respectively. RNAsin was from Promega (Madison, WI, USA).

Cloning and *in vitro* transcription of synthetic yeast $tRNA^{His}$ genes

Ten synthetic overlapping deoxyoligonucleotides, corresponding to the consensus sequence of the T7 RNA polymerase promoter and to the sequence of yeast $tRNA^{His}_1$ (23) were hybridized and inserted into pUC119 linearised with *Bam*HI and *Hind*III as described for yeast $tRNA^{Asp}$ synthetic gene (24). An *Eco*T22I restriction site was introduced instead of *Bst*NI since there is an internal *Bst*NI restriction site in the tRNA sequence. Three variants of the $tRNA^{His}$ gene were cloned by replacing two overlapping oligonucleotides with their corresponding mutated versions. Transcriptions of these genes yield $tRNA^{His}$ transcripts with either a deletion of residue G at position −1, a mutation at position 36 (G into C) or a mutation at position 73 (A into G). Transcriptions of $tRNA^{His}$ genes (wild-type and mutated) were performed by incubation of *Eco*T22I-linearised plasmid (8 μg) with 450 units of T7 RNA polymerase in 40 mM Tris–HCl pH 8.0, 22 mM $MgCl_2$, 1 mM spermidine, 5 mM dithioerythritol, 0.01% Triton X100, 120 units RNAsin, 4 mM of each nucleoside triphosphate and 16 mM GMP in 150 μl for 3 hours at 37°C. After phenol extraction, transcripts were ethanol precipitated and purified to nucleotide resolution on denaturing 12% polyacrylamide/8 M urea gels. The full length transcripts were electroeluted from the gel using a Biotrap electroelution apparatus (Schleicher and Schuell, Dassel, Germany), ethanol precipitated, washed and dissolved in water.

Cloning and *in vitro* transcription of synthetic yeast $tRNA^{Asp}$ genes

Plasmids containing synthetic genes of wild-type and mutant $tRNA^{Asp}$ downstream of a T7 RNA polymerase DNA dependent transcriptional promoter, were prepared as described elsewhere (24). They contain a *Bst*NI restriction site at the precise end of the sequence encoding the tRNA. In order to permit transcription of these synthetic genes, base-pair $U_1 \cdot A_{72}$ was replaced by $G_1 \cdot C_{72}$ (24). Transcripts were synthesized by incubation of *Bst*NI-linearised plasmid (15 μg) with 450 units of T7 RNA polymerase in the same reaction mixture as for $tRNA^{His}$.

Cloning and *in vitro* transcription of minihelices

Plasmid pTYAA encoding the amino acid accepting arm of the tRNA-like structure present at the 3′ end of the Turnip Yellow Mosaic Virus RNA, adjacent to the T7 RNA polymerase promoter was created by oligonucleotide-directed mutagenesis of clone pTYAlu as described earlier (18). *In vitro* transcription of this plasmid leads to $TYA_4 \cdot U_{22}$. Variants of this molecule were obtained by *in vitro* transcription of synthetic genes constructed with overlapping oligonucleotides and cloned according to established methods (24). Transcription was performed in the same conditions as for yeast $tRNA^{Asp}$. Full-length transcripts were purified on 16% preparative polyacrylamide gels and electroeluted as described for $tRNA^{His}$ transcripts.

Aminoacylation assays and interpretation of kinetic data

Aminoacylation assays were performed at 30°C in 55 mM Tris–HCl pH 7.5, 15 mM $MgCl_2$, 10 mM ATP, 2.5 mM glutathione, 30 mM KCl, 25 μM L-[^{14}C] histidine and the required concentrations of transcript and yeast HisRS. Aliquots were spotted on 3MM Whatman paper at different times and 5% trichloroacetic acid precipitated. Incorporation of radioactive aminoacid was measured by liquid scintillation spectroscopy. Kinetic parameters (K_M and V_{max}) were determined from Lineweaver–Burk plots.

The efficiency of aminoacylation of variants respective to the transcript considered as control was appreciated by comparison of the ratios (V_{max}/K_M). Thus, $(V_{max}/K_M)_{relative} = (V_{max}/K_M)_{variant}/(V_{max}/K_M)_{control}$. A more intuitive number, ***L***, indicates the loss in aminoacylation efficiency of a variant as compared to the control. It corresponds to the inverse of $(V_{max}/K_M)_{relative}$ (25, 26). Conversely, ***G***, corresponds to the gain in efficiency of a variant as compared to a control and is calculated by the ratio between $L_{control}/L_{variant} \cdot V_{max}/K_M$ values are averages of three independent experiments; errors on ***L*** and ***G*** values are about 20%.

RESULTS AND DISCUSSION

Importance of residues G_{-1} and A_{73} for histidine identity in yeast

Extra nucleotide G_{-1}. As occurs throughout all organisms, yeast histidine specific tRNAs differ from other cellular tRNAs by the presence of an additional residue at their 5′-end (15). Since this feature is unique and is already known to specify histidylation in *E.coli*, it represents the most obvious candidate for a major identity element in yeast tRNAs. To test this prediction, a

$tRNA^{His}$ transcript lacking G_{-1} was generated (Fig. 1). As expected, the deleted variant shows its catalytic efficiency for histidylation, estimated by the V_{max}/K_M ratio, decreased 470-fold as compared to the wild-type $tRNA^{His}$ transcript (Table 1). This loss is mainly due to a decrease of V_{max} (106-fold), K_M being only weakly affected (4-fold).

Discriminator base 73. Discriminator nucleotide at position 73, opposite to base G_{-1}, is always an A in yeast $tRNA^{His}$ isoacceptors. Because of the frequent involvement of the discriminator position in tRNA identity and of the uniqueness of A_{73} in yeast $tRNA^{His}$ isoacceptors, we considered this position as a potential histidine identity element. Since the discriminator position in eukaryotic $tRNA^{His}$ species is always occupied by a purine (15), a G_{73} variant of yeast $tRNA^{His}$ was generated (Fig. 1). Its histidine charging ability is significantly affected with a V_{max}/K_M value 22-times lower than for the wild-type $tRNA^{His}$ transcript. Again, this loss in catalytic efficiency is mainly due to a reduced V_{max} (Table 1).

First conclusions and their implications. The above mutational analysis of $tRNA^{His}$ indicates the primordial role of residue G_{-1} and to a lesser extent of discriminator residue A_{73} in histidine identity in yeast. This conclusion for a eukaryotic system is reminiscent to what is found for prokaryotic $tRNA^{His}$ identity (11), with the exception that the discriminator residue in prokaryotes (and organelles) is always a pyrimidine instead of a purine in eukaryotes (15). Explicit proof of the role in identity of these two residues requires transplantation experiments in other tRNA frameworks. In what follows G_{-1} and A_{73} have been transplanted into two alternate RNA frameworks namely part of the tRNA-like domain of TYMV RNA and yeast $tRNA^{Asp}$. Moreover, the differences between prokaryotes and eukaryotes was further investigated by studying the influence of pyrimidines at position 73.

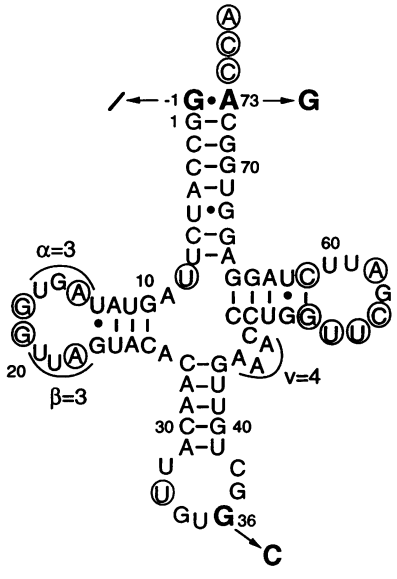

Figure 1. Cloverleaf sequence of yeast $tRNA_1His$ transcript. Residues that have been mutated or deleted are indicated in bold. Conserved nucleotides in all tRNAs are circled. The lengths of the a and b regions in the D-loop and the number of residues forming the variable loop are given. Unusual base pairings are symbolized by dots.

Histidylation by yeast HisRS of minihelices derived from the TYMV tRNA-like structure

Structural and functional background. In our view a tRNA structure represents a scaffolding selected by nature to present identity nucleotides optimally toward the synthetase (1, 27). Thus, we have chosen to study the expression of nucleotides -1 and 73 in a RNA context markedly different from that of a canonical tRNA. This was possible because we already demonstrated that a minihelix derived from the TYMV tRNA-like structure can be charged by yeast HisRS (18). Such a minihelix contains a pseudoknot (Fig. 2). The reason accounting for its histidylation was suggested to rely in the mimicry between nucleotide U_{22} from the pseudoknot and residue G_{-1} in a canonical tRNA, which makes pairing with discriminator residue A_4 as well as stacking of these two residues over the amino acid accepting branch (20, 28) possible. Considering the potential of this pseudoknotted structure to mimic a $N_{-1} \cdot N_{73}$ pair, we mutated the minihelix at both positions 22 (the analog of residue -1) and 4 (the analog of the discriminator base), to create in the tRNA-like context, the wild-type $G_{22} \cdot A_4$ mismatch of yeast $tRNA^{His}$. In addition we created the three variants ($G_{22} \cdot N_4$, named TY-$G_{22} \cdot N_4$) with mutations at the discriminator position and the other three variants ($N_{22} \cdot A_4$, named TY-$N_{22} \cdot A_4$) in which the G_{-1} mimic is changed (Fig. 2). From a practical point of view, it is noticeable that preparation of these variants with the T7 methodology is straightforward in contrast to what would occur in canonical tRNAs where the most 5′-residue has to be a G residue for efficient transcription by T7 RNA polymerase (29).

Mutation at positions equivalent to N_{-1} and N_{73}. If the $G_{-1} \cdot A_{73}$ mismatched pair is a major histidine identity element in yeast, the minihelix TY-$G_{22} \cdot A_4$ shown in Figure 2 should be a better substrate for HisRS than the wild-type TY-$U_{22} \cdot A_4$ minihelix, already known to be histidylable (18). In contrast to our earlier experiments, where conditions giving rise to optimal charging of the minihelix were used, we took in the present work the same

Table 1. Kinetic parameters for histidylation of various transcripts derived from yeast $tRNA^{His}$. The sequence of residues $-1 \cdot 73$ is given explicitly in brackets for each transcript

Transcript	Level of charging (%)	K_M (μM)	V_{max} (arbitrary units)	V_{max}/K_M (arbitrary units)	L^a relative to transcript^{His} (x-fold)	
$tRNA^{His}$(wt)	[G·A]	70	0.8	2650	3310	1
$tRNA^{His}$	[/·A]	57	3.6	25	7	470
$tRNA^{His}$	[G·G]	40	1.0	150	150	22
$tRNA^{His}C36$	[G·A]	33	0.8	1335	1670	2

[a]L corresponds to losses of efficiency.

aminoacylation conditions as for optimal $tRNA^{His}$ charging. These conditions are less favourable for minihelix histidylation. aminoacylation conditions as for optimal $tRNA^{His}$ charging. These conditions are less favourable for minihelix histidylation.

As expected, charging levels up to 26% were obtained with the TY-$G_{22}\cdot A_4$ minihelix, whereas histidylation plateaus reached only 4% with TY-$U_{22}\cdot A_4$ transcript (Table 2). This corresponds to an increase in catalytic efficiency of 9-fold. Variants with A_{22} and C_{22}, present a loss of their catalytic efficiency of 5- and 30-fold, respectively, as compared to TY-$G_{22}\cdot A_4$. For all three minihelices with decreased activity as compared to TY-$G_{22}\cdot A_4$, the reduced histidylation is exclusively due to a V_{max} effect. These kinetic results confirm that G_{-1} has its equivalent at position 22 in the minihelix derived from the TYMV tRNA-like structure and show that this position has to be occupied by a G residue for optimal histidylation by the yeast enzyme. Conversely, these functional data are another proof of the existence of the pseudoknotted fold in the TYMV derived minihelices.

In a second step, we mutated the equivalent of the discriminator base (A_4 in the wild-type minihelix) into a G, a C or an U residue while keeping a G residue at position 22 (Fig. 2). Here, the aim was to investigate the specific role played by the chemical nature of residue 73 in histidylation. Transcripts TY-$G_{22}\cdot C_4$ and TY-$G_{22}\cdot U_4$ exhibit losses in histidylation efficiency of only 9- and 5-times, respectively, as compared to TY-$G_{22}\cdot A_4$. These losses are relatively moderate when compared to that determined for mutant TY-$G_{22}\cdot G_4$ which is 59-fold reduced (Table 2).

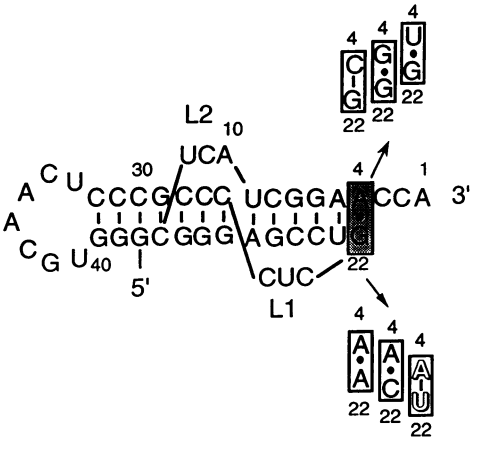

Figure 2. Minihelix TY-$G_{22}\cdot A_4$ derived from the amino acid acceptor arm of TYMV tRNA-like structure with a $G_{22}\cdot A_4$ pair (shaded) mimicking the $G_{-1}\cdot A_{73}$ pair of yeast $tRNA^{His}$. In the wild-type TYMV RNA, this base-pair is $U_{22}\cdot A_4$ (large lettering). As usual in viral tRNA-like structures, nucleotides are numbered from the 3'-end. L1 and L2 refer to the single stranded loops connecting the different helices of the molecule. Five variants with mutations at pair $N_{22}\cdot N_4$ were created. The exact sequence of these pairs are given explicitly in the different squares.

Altogether these kinetic experiments show that the best substrate for histidylation by yeast HisRS is TY-$G_{22}\cdot A_4$ which presents the same nucleotides at the end of its amino acid acceptor stem as yeast $tRNA^{His}$ isoacceptors. The functional transplantation of base-pair $G_{22}\cdot A_4$ indicates further that the non-canonical structural framework of TYMV RNA is not detrimental for interaction with yeast HisRS. Thus, histidylation by yeast HisRS follows the same rules as in *E.coli* (11), namely a sequence dependent recognition of the very terminal part of the tRNA amino acid acceptor stem.

Minihelix TY-$G_{22}\cdot A_4$ shows a loss in histidylation efficiency of about four orders of magnitude as compared to wild-type $tRNA^{His}$. This observation is in contrast to what was observed for the *E.coli* microhelix^{His} which is only 150-times less well histidylated than the entire $tRNA^{His}$ (13). Since the molecules studied in this work are not directly derived from yeast $tRNA^{His}$, it may be that they lack some minor identity signals and/or present antideterminants (e.g. elements from the pseudoknotted fold) hindering optimal recognition by yeast HisRS. This last possibility appears indeed the most likely since experimental conditions (e.g. addition of $MgCl_2$) affecting RNA conformation enhance significantly the level of charging, likely as the result of a better structural adaptation of the minihelices to the enzyme (18).

Transplantations in the aspartate context

Choice of the host tRNA. To further verify the importance of residues −1 and 73 in yeast histidine identity, we transplanted residues G_{-1} and A_{73} into yeast $tRNA^{Asp}$ (Fig. 3). The choice of this tRNA was dictated by its structural similarity with yeast $tRNA^{His}$. Indeed, this is an important prerequisite since it has been shown that conformational features modulate expression of identity sets (7–9). Both $tRNA^{Asp}$ and $tRNA^{His}$ possess a 4 nucleotide-long variable region, as well as a and b domains of identical length (see Figs. 1 and 3). Thus, it is expected *a priori* that the overall conformation of the new host tRNA should not perturb the expression of histidine identity.

Histidylation of wild-type yeast $tRNA^{Asp}$ transcript. As a control, wild-type $tRNA^{Asp}$ transcripts were investigated for histidylation. Surprisingly, these transcripts are recognized and

Table 2. Kinetic parameters for histidylation of various transcripts derived from minihelix TY-$G_{22}\cdot A_4$. The sequence of pair 22·4 (equivalent to pair −1·73 in yeast $tRNA^{His}$) is given explicitly for each minihelix

Transcript	Level of charging (%)	K_M (μM)	V_{max} ($\times 10^3$) (arbitrary units)	V_{max}/K_M ($\times 10^3$) (arbitrary units)	L^a relative to TY-$G_{22}\cdot A_4$ (x-fold)
TY-$G_{22}\cdot A_4$	26	17	5000	294	1
TY-$A_{22}\cdot A_4$	4	20	1200	60	5
TY-$C_{22}\cdot A_4$	2	17	165	10	30
TY-$U_{22}\cdot A_4$*	4	20	665	33	9
TY-$G_{22}\cdot C_4$	8	33	1100	33	9
TY-$G_{22}\cdot G_4$	1	7	34	5	59
TY-$G_{22}\cdot U_4$	9	20	1100	55	5

[a]*L* corresponds to losses of efficiency. *Corresponds to the wild-type sequence of TYMV RNA.

significantly charged by yeast HisRS (Table 3). Up to 13% of the molecules can be aminoacylated under standard aminoacylation conditions, but with a catalytic efficiency reduced 16600-fold as compared to wild-type $tRNA^{His}$ transcript. This decrease results predominantly from a V_{max} effect (8800-fold). The capacity of yeast $tRNA^{Asp}$ transcript to be weakly histidylated is obviously relevant to the presence of one or more weak histidine identity elements (most probably present in the consensus sequence between yeast $tRNA^{His}$ and yeast $tRNA^{Asp}$, and which concerns 42% of the nucleotides non-conserved in all tRNAs). The common conformational characteristics of both tRNAs combined to the absence of modified bases that relax tRNA structure (24, 30), contribute probably also with the capacity of yeast $tRNA^{Asp}$ transcript to be mischarged by yeast HisRS.

Histidylation of single variants. The three yeast $tRNA^{Asp}$ transcripts in which histidine specific nucleotides have been inserted are displayed in Figure 3. Addition of nucleotide G_{-1}

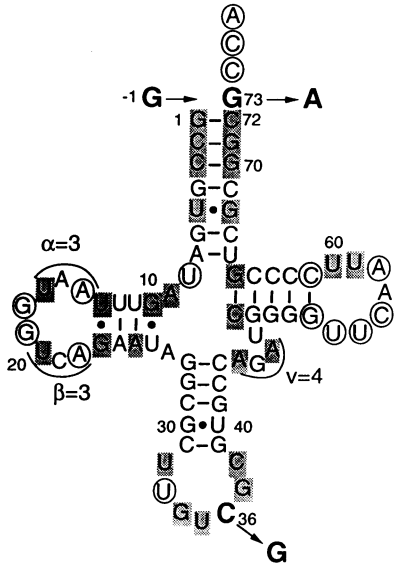

Figure 3. Cloverleaf sequence of yeast $tRNA^{Asp}$ transcript. Residues that were mutated or added are indicated in bold. Nucleotides common to both yeast $tRNA^{Asp}$ and yeast $tRNA_1His$ transcripts are shaded whereas conserved residues in all tRNAs are circled. The lengths of the a and b regions in the D-loops and the number of residues forming the variable loops are given. As discussed in Materials and Methods, the $tRNA^{Asp}$ transcript possesses a $G_1 \cdot C_{72}$ instead of an $U_1 \cdot A_{72}$ base-pair.

at the 5'-terminus of $tRNA^{Asp}$ enhances markedly its histidylation capacity. About 43% of the variant can be charged by yeast HisRS. The K_M is approximativly the same as for yeast $tRNA^{His}$ whereas V_{max} is 63-fold decreased (Tables 1 and 3). Thus, this variant of $tRNA^{Asp}$ is 70-fold less efficiently histidylated than the $tRNA^{His}$ transcript, but becomes a 230-times better substrate for HisRS than the wild-type $tRNA^{Asp}$ transcript (Table 3). This transplantation experiment confirms the involvement of nucleotide G_{-1} in the identity of yeast $tRNA^{His}$.

Transplantation of histidine identity element A_{73} into yeast $tRNA^{Asp}$ enhances also its histidylation properties. This transcript is charged to a plateau level of 37% whereas the wild-type G_{73} $tRNA^{Asp}$ molecule is only charged to 13% (Table 3). Here also, the 5-fold improvement of histidylation efficiency is due to a V_{max} increase. This effect is moderate and points to a minor role played by the discriminator nucleotide A_{73} in histidine identity.

The anticodon region in histidine specific tRNAs should not *a priori* contain strong histidine identity elements because of the predominant role of the amino acid acceptor stem in this identity, well accounted for by the charging of histidine minimalist RNA substrates (this work and *e.g.* refs 13, 14, 18). However, anticodon loops of yeast $tRNA^{Asp}$ and $tRNA^{His}$ share exactly the same sequence except at position 36 which is occupied by a guanine in $tRNA^{His}$ and by a cytosine in $tRNA^{Asp}$ (see Figs. 1 and 3). Thus, introduction of G_{36} in $tRNA^{Asp}$ gives rise to a chimeric tRNA molecule identical to $tRNA^{His}$ at the anticodon loop level. Histidylation of this mutant is only 2-times more efficient than wild-type $tRNA^{Asp}$ (Table 3), showing a very low contribution of position 36 in yeast histidine identity. To directly prove this conclusion, the complementary experiment was performed in which a yeast $tRNA^{His}$ transcript bearing a C_{36} in the anticodon was tested in histidylation. As could be expected, the V_{max}/K_M of this mutant was only 2-fold decreased as compared to the wild-type $tRNA^{His}$ (Table 1).

Histidylation of $tRNA^{Asp}$ double mutant $G_{-1} \cdot A_{73}$. The previous results have shown that both nucleotides G_{-1} and A_{73} contribute to histidine identity although with different strengths. In order to cumulate the beneficial effect brought by these two residues and to obtain a more efficient substrate for yeast HisRS, a double mutant derived from the $tRNA^{Asp}$ sequence was created presenting simultaneously G_{-1} and A_{73} at the top of the amino acid acceptor stem. In the case of an additional behaviour of the two identity elements, a 1000-fold gain (***G***) in histidylation efficiency of the transplanted $tRNA^{Asp}$ is expected [$G = 230 \times 5$, indeed, a ***G*** of 230-fold is expected to occur after

Table 3. Kinetic parameters for histidylation of transplanted yeast $tRNA^{Asp}$. The sequence of residues $-1 \cdot 73$ is given explicitly in brackets for each molecule

Transcript		Level of charging (%)	K_M (μM)	V_{max} ($\times 10^3$) (a.u.)	V_{max}/K_M ($\times 10^3$) (a.u.)	***L***[a] relative to transcript^{His} (x-fold)	***G***[b] relative to transcript^{Asp} (x-fold)
$tRNA^{Asp}$(wt)	[/·G]	13	1.5	300	200	16600	1
$tRNA^{Asp}$	[G·G]	43	0.9	42000	46700	70	230
$tRNA^{Asp}$	[/·A]	37	2.4	2300	960	3450	5
$tRNA^{Asp}$G36	[/·G]	30	2.7	1200	445	7440	2
$tRNA^{Asp}$	[G·A]	35	4.0	25600	6400	520	30

[a]***L*** corresponds to losses of efficiency and [b]***G*** corresponds to gains of efficiency.
a.u.: arbitrary units.

insertion of nucleotide G_{-1} and a *G* of 5-fold after insertion of residue A_{73} ; in the case of additive effects, the total gain of efficiency is the product of both individual gains, in that of cooperative or anti-cooperative effects of both mutations, the total gain in efficiency is different (25, 26)]. Surprisingly, the double mutant is only 30-times better histidylated than yeast $tRNA^{Asp}$ transcript. This reflects a strong anti-cooperative behaviour of the G_{-1} and A_{73} histidine identity elements in the $tRNA^{Asp}$ context. This anti-cooperative effect is also illustrated when comparing the strong loss of histidylation efficiency of the $tRNA^{Asp}$ double mutant to $tRNA^{His}$ (L = 520). A likely interpretation for the anti-cooperative properties of this $tRNA^{Asp}$ double mutant may be a non-optimal presentation of the $G_{-1} \cdot A_{73}$ histidine identity elements towards yeast HisRS in the $tRNA^{Asp}$ context. This would lead to an incorrect orientation of the CCA terminus, reflected by the major contribution of V_{max} in the loss of specificity. At the present stage of our investigations, we cannot distinguish between the precise possible structural reasons of this effect. It could be due to faint differences in the conformation of the amino acid acceptor stems of $tRNA^{Asp}$ and $tRNA^{His}$ (notice however the high homology of these regions in both tRNAs), but more likely could arise from more global changes linked to differences in the tertiary interaction networks in both tRNAs. An explicit example where the nature of nucleotides in a tertiary interaction is important for identity has been demonstrated in the case of *E.coli* $tRNA^{Cys}$ with the involvment of the unusual $G_{15} \cdot G_{48}$ Levitt base-pair (10). Further tRNA engineering experiments will unravel this problem in the histidine system.

GENERAL CONCLUSIONS

This work illustrates the limitation of the transplantation approaches, in which the reality of identity elements is demonstrated by their effective expression in another tRNA sequence. Although this approach proved to be extremely useful in many instances (e.g. 31−34), it did not always allow optimal expression of an identity set in a new tRNA context. This was shown in several cases (e.g. 7−9) and is further illustrated here with the transplantation of histidine identity elements into yeast $tRNA^{Asp}$. Poor activities, corresponding phenomenologically to anti-cooperative effects, are due either to antideterminants effects and/or to subtle conformational differences between the various tRNAs. Nature retained optimal structural scaffoldings during evolution to ensure optimal specificity of tRNA aminoacylation reactions.

This paper shows that the identity of $tRNA^{His}$ in yeast is ensured essentially by a similar molecular strategy as in prokaryotes studied so far (*E.coli*), namely a role for residues −1 and 73. The major histidine identity element in yeast is residue G_{-1}, whose effect is correlated with that of the discriminator residue 73. Anticodon-loop nucleotides are likely not involved in histidine identity. Interestingly, yeast HisRS recognizes residues G_{-1} and A_{73} in particular substrates. We have shown previously that a minihelix corresponding to the aminoacyl acceptor arm of the tRNA-like domain of TYMV is efficiently charged with histidine (18). Here we demonstrate that this aminoacylation specificity is directly linked to the presence of residues mimicking nucleotides G_{-1} and A_{73} from yeast $tRNA^{His}$, confirming the role of these nucleotides in histidine identity. Thus, HisRS recognizes its specific identity elements whether they are presented in a classical RNA helix or in a particular folding of an RNA chain as is the case in the TYMV derived minihelix where a pseudoknot occurs.

Because histidine identity in prokaryotes is dependent upon the presence of residue C_{73} whereas in eukaryotes it is dependent upon the presence of A_{73}, it can be suggested that the discrimination between histidine specificity in both kingdoms is linked to the nature of the discriminator base. As far as minor histidine elements are concerned, it is interesting to notice that all the RNA substrates studied in this work contain the same base-pairs at positions 2·71 and 3·70 as in *E.coli* tRNA where these pairs have been found as minor identity elements (14).

It is worth mentioning that yeast HisRS histidylates also the tRNA-like structure of tobacco mosaic virus (16, 21), that of the satelite of this virus (19), as well as that of brome mosaic virus and a series of derived mini-substrates (20). The common feature of these substrates and of those studied in this work is the presence of a nucleotide mimicking a −1 residue. The nature of this −1 residue is variable since all four nucleotides allow histidylation although at variable efficiencies. The outcome of these observations is that histidine identity primarily requires a structural information in its substrate, the presence of a residue at position −1. Because this residue is mimicked by an internal nucleotide in the pseudoknot containing substrate, it can be concluded that this residue has to be stacked on top of the accepting helix and likely that the tRNA does not undergo drastic conformational changes at this level during aminoacylation. The fact that HisRS belongs to class II synthetases (35) agrees with this view. Indeed, in the representative class II $tRNA^{Asp}$/AspRS complex structure (36), the tRNA maintains its initial conformation in the aminoacid accepting stem in contrast to what happens in a class I complex (37). Optimal expression of the histidine identity is ensured by the adequate sequence combination between residues −1 and 73. Following this view, it is understandable that other combinations than those found in the natural $tRNA^{His}$ substrate of yeast HisRS are found in the viral tRNA-like molecules which have not been optimized for a yeast system.

ACKNOWLEDGEMENTS

We thank Dr F.W.Studier (Brookhaven) for providing the T7 polymerase overproducing strain and Drs M.Frugier and A.Théobald-Dietrich for help in DNA cloning. This work was supported by grants from the Centre National de la Recherche Scientifique (CNRS), Ministère de la Recherche et de la Technologie (MRT) and by Université Louis Pasteur (Strasbourg).

REFERENCES

1. Giegé, R., Puglisi, J.D. and Florentz, C. (1993) *Prog. Nucleic Acid Res. Mol. Biol.*, **45**, 129−206.
2. McClain, W.H. (1993) *J. Mol. Biol.*, **234**, 257−280.
3. Saks, M.E., Sampson, J.R. and Abelson, J.N. (1994) *Science*, **263**, 191−197.
4. Muramatsu, T., Nishikawa, K., Nemoto, F., Kuchino, Y., Nishimura, S., Miyazawa, T. and Yokoyama, S. (1988) *Nature*, **336**, 179−181.
5. Perret, V., Garcia, A., Grosjean, H., Ebel, J.P., Florentz, C. and Giegé, R. (1990) *Nature*, **344**, 787−789.
6. McClain, W.H. and Foss, K. (1988) *Science*, **241**, 1804−1807.
7. Perret, V., Florentz, C., Puglisi, J.D. and Giegé, R. (1992) *J. Mol. Biol.*, **226**, 323−333.
8. Frugier, M., Florentz, C., Schimmel, P. and Giegé, R. (1993) *Biochemistry*, **32**, 1405- 14061.
9. Rogers, K.C. and Söll, D. (1993) *Biochemistry*, **32**, 14210−14219.

10. Hou, Y.M., Westhof, E. and Giegé, R. (1993) *Proc. Natl. Acad. Sci. U.S.A.*, **90,** 6776–6780.
11. Himeno, H., Hasegawa, T., Ueda, T., Watanabe, K., Miura, K. and Shimizu, M. (1989) *Nucleic Acids Res.*, **17,** 7855–7863.
12. Yan, W. and Francklyn, C. (1994) *J. Biol. Chem.*, **269,** 10022–10027.
13. Francklyn, C. and Schimmel, P. (1990) *Proc. Natl. Acad. Sci. U.S.A.*, **87,** 8655–8659.
14. Francklyn, C., Shi, J.P. and Schimmel, P.,(1992) *Science*, **255,** 1121–1125.
15. Steinberg, S., Misch, A. and Sprinzl, M. (1993) *Nucleic Acids Res.*, **21,** 3011–3015.
16. Oberg, B. and Philipson, L. (1972) *Biochem. Biophys. Res. Commun.*, **48,** 927–932.
17. Garcia-Arenal, F. (1988) *Virology*, **167,** 201–206.
18. Rudinger, J., Florentz, C., Dreher, T. and Giegé, R. (1992) *Nucleic Acids Res.*, **20,** 1865–1870.
19. Felden, B., Florentz, C., McPherson, A. and Giegé, R. (1994) *Nucleic Acids Res.*, **22,** 2882–2886.
20. Felden, B. (1994) Thèse de l'Université Louis Pasteur, Strasbourg, France.
21. Mengual, R . (1977) Thèse de l'Université Louis Pasteur, Strasbourg, France.
22. Wyatt, J.R., Chastain, M. and Puglisi, J.D. (1991) *BioTechniques*, **11,** 764–769.
23. Keith, G., Pixa, G., Fix, C. and Dirheimer, G. (1983) *Biochimie*, **65,** 661–672.
24. Perret, V., Garcia, A., Puglisi, J., Grosjean, H., Ebel, J., Florentz, C. and Giegé, R. (1990) *Biochimie*, **72,** 735–744.
25. Fersht, A. (1985) *Enzyme, Structure and Mechanism.* Freeman, New-York.
26. Pütz, J., Puglisi, J.D., Florentz, C. and Giegé, R. (1993) *EMBO J.*, **12,** 2949–2957.
27. Giegé, R., Florentz, C. and Dreher, T.W. (1993) *Biochimie*, **75,** 569–582.
28. Dumas, P., Moras, D., Florentz, C., Giegé, R., Verlaan, P., Van Belkum, A. and Pleij, C.W.A. (1987) *J. Biomol. Struct. Dyn.*, **4,** 707–728.
29. Milligan, J.F., Groebe, D.R., Witherell, G.W. and Uhlenbeck, O.C. (1987) *Nucleic Acids Res.*, **15,** 8783–8798.
30. Sampson, J.R. and Uhlenbeck, O.C. (1988) *Proc. Natl. Acad. Sci. U.S.A.*, **85,** 1033–1037.
31. Schulman, L.H. and Pelka, H., (1988) *Science*, **242,** 765–768.
32. Sampson, J.R., DiRenzo, A.B., Behlen, L.S. and Uhlenbeck, O.C. (1989) *Science*, **243,** 1363–1366.
33. Pütz, J., Puglisi, J.D., Florentz, C. and Giegé, R. (1991) *Science*, **252,** 1696–1699.
34. Normanly, J., Ollick, T. and Abelson, J. (1992) *Proc. Natl. Acad. Sci. U.S.A.*, **89,** 5680-5684.
35. Eriani, G., Delarue, M., Poch, O., Gangloff, J. and Moras, D. (1990) *Nature*, **347,** 203–206.
36. Ruff, M., Krishnaswamy, S., Boeglin, M., Poterszman, A., Mitschler, A., Podjarny, A., Rees, B., Thierry, J.C. and Moras, D. (1992) *Science*, **252,** 1682–1689.
37. Rould, M.A., Perona, J.J., Söll, D. and Steitz, T.A. (1991) *Science*, **246,** 1135–1142.